

**Characterization
of Automotive Color
and Appearance**



Characterization of Automotive Color and Appearance utilizing an under-sampled BRDF (bi-directional reflectance differential function) and new hand held Multi-angle Spectrophotometry

Colored plastics are complex chemical compositions involving advanced processes that continue to innovate and evolve. Adopting nano-materials and micro-technologies processes and controls, creative engineers have developed systems that allow lower cost and innovative color styling, while evoking the emotional response desired by the designer.

Traditional spherical and in-plane spectrophotometric measurements are insufficient when characterizing modern colored plastics. This paper presents a novel combination of spatial under sampled BRDF (including out of plane geometry) and a simple phenomenological model that captures both nanoscale and microscale formulation contributions as well as process related contributions to overall appearance. Presented are preferable spectrophotometric sampling geometries as well as examples of formulation, lot to lot distribution variations, process variations, and separability of contributors.

Background Information

For materials where gloss, texture and other effects play an important role, the process of selection, definition and production control is still based on physical samples and visual assessment. Traditional color measurement and communications methods do not directly support production process control and root cause error detection. Textured and patterned nacreous pigments in plastics are some of the areas that could benefit from a digital means to define, communicate, and render appearance.

Visual appearance consists of both detection and inference. It extends spectral reflectance at a point into the context of an observation. It includes assumptions regarding illumination and observation as well as physical conditions of the sample such as shape and texture. At the outset, our work set out to provide a basis for a reliable color process using spectral color definition and communication. However, to do this we needed a method for translating the abstract concepts of color appearance into a concrete expressive model. Our research currently underway seeks to extend this paradigm to a more comprehensive definition of total appearance that includes context and inference.

Starting from a measurement perspective, fundamentally we have a spectro-radiometer. A source is directed towards an object through a given Optical Transfer Function (OTF). The light impinging on the ob-

ject interacts through each layer and interface of the object guided by Maxwell's equations and undergoes Mie and Rayleigh scattering. From here, the resultant Bidirectional Reflectance Distribution Function (BRDF) or Bidirectional Subsurface Scatter Reflectance Distribution Function (BSSRDF) is sampled from a given observation direction. This set of BRDF samples is collected by an optical system having a second OTF. We then sense the resultant OTF and transform it in terms of Context (described and defined later). Once the information has been processed for Context there is the final step involving inference which enables creation, communication, and decision making.

The challenge associated with measurement of the BRDF of a sample is with the time associated with performing many Goniometric measurements, as many different illumination and observation angles/geometries are required. Our research was focused on hand held measurement and devices, and typically is it difficult to hold such an instrument steady for more than 1-1 1/2 seconds. Therefore, a rigorous deterministic measurement requires more illumination/observation pairs than is possible in the allowable time. How does an undersampled measurement relate to such a closed form solution? What angles are important? What spectral information is important?

Our appearance measurement platform reported in this paper consists of a compact multi-angle spectrophotometer system combined with sparse sampling of directional reflectance spectra for traditional BRDF (As shown in figure 1). A dielectric filter based diode spectrophotometer design overcomes the dynamic range and accuracy limitations of other approaches and provides backwards correlation to existing in plane geometries. Illumination and measurement from multiple out of plane angles yields a rich data set that is capable of providing a complete description of the surface appearance. The common platform has been used to derive a family of instruments aimed at users from design to production.

The sampling of the various BRDF functions as they are generated defines the resultant response used to quantify Appearance. Multi-Angle spectroscopic measurements produce large amounts of data. To make this data tractable, rigorous physical models are applied to estimate the parametric descriptors for surface appearance. Research



in optics, electromagnetics, computer graphics, and vision has resulted in significant advances in the area of surface appearance modeling. These models have been evaluated and refined for applicability to industrial samples and applications. A suite of reflectance models for BRDF and texture parameterization have been developed to describe surface appearance. These descriptors (model parameters) are transported as XML to provide the backbone for a digital surface appearance process from concept to creation. See Figure 2.

The BRDF data can be derived from the goniometric spectrometer measurements by applying the data to the following expression:

$$L_r(x, \omega) = \int_{\Omega_x} f_r(x, \omega', \omega) L_i(x, \omega') (n \cdot \omega) d\omega'$$

where L_r is the reflected radiance at x in direction ω . x is the hemisphere of incoming directions, f_r is the BRDF at x and in our case contains both a specular/glossy term f_r^S and a diffuse term f_r^D such that:

$$f_r(x, \omega', \omega) = f_r^S(x, \omega', \omega) + f_r^D(x, \omega', \omega)$$

L_i is the incoming radiance and can be related to the flux by:

$$L_i(x, \omega') = d^2\Phi_i(x, \omega') / (n \cdot \omega') d\omega' dA_i$$

In the case of a multilayer photon transport model, the form of the volumetric rendering equation is significantly different than above and must consider both the optical depth for each scattering layer as well as a phase function describing the nature of the scattering function. The equation takes the form:

$$L_r(x, \omega) = \int_0^s e^{-\kappa(x, x')} a(x') L_e(x', \omega) dx' + \int_0^s e^{-\kappa(x, x')} s(x') \int_{\Omega} \omega \cdot \omega' p(x, \omega', \omega) L_i(x, \omega') d\omega' dx' + e^{-\kappa(x, x+s)} L(x-s, \omega)$$

where the optical depth $\kappa(x, x')$ is given by:

$$\kappa(x, x') = \int_x^{x'} \kappa(t) dt$$

and the phase function can take various different forms depending on the structure of the coating and the nature of the dominant scattering material. The most commonly used phase function is the Henyey-Greenstein phase function which can be used in a combination with differences for each layer and/or scattering component. It takes the generalized form:

$$p(\omega) = N \sum_{i=1}^m w_i (1-g_i^2) / (4\pi(1+g_i^2-2g_i \cos\theta)^{1.5}) \text{ where } \sum w_i = 1$$

Where, g_i controls the shape of each lobe and w_i the weight. Depending on the complexity of the coating, the context for the sampling, and the intended inference to be made, as many as 72-90 measurement angles (channels) are required for complete BSSRDF

formulation of a 3-4 layer coating such as an automotive paint. In the other extreme, as few as 10-12 angles are required for BRDF based measurement of a homogeneous plastic where differences in formulation and process (and not pure formulation) are of primary concern.

Objective of work

Existing industry standards for measuring colored plastics consist of either spherical or in-plane goniometric spectrophotometer measurements. The problem with this approach is that today's complex plastics are 3 dimensional in nature. The contribution of the plastic formulation to perception changes in the out of plane direction. Traditional in plane geometries and single camera systems do not account for the fact that perceptual effects are goniometric in nature. They change with varying illumination and observation conditions. Today we do not measure appearance with a sphere, we just average it up. Appearance variations due to molecular alignment are perceptual effects. Today we only measure the average scatter and reflection of the light with the sample. Because the resulting BRDF (BSSRDF) varies multidimensionally, so will the perceptual effects such as Texture and molecular alignment. Today's systems are not capable of robustly characterizing and communicating the impact of process and formulation variation on perceptual effects. It is our objective to present a cost effective hardware and software solution for doing this.

Experimental procedure

There are two unique properties of light's interaction with material that can be exploited in the measurement process to learn and understand more about the structure and makeup of a material (or coating). The first property that we can consider is the fact that all materials are dispersive. By this we mean that the ability of a material to bend light (it's refractive index) is different for blue light (400nm) than it is for red light (700nm). This change in bending power exists regardless the apparent color (absorptive property) of the material. Even a material that appears black or shiny (like a mirror) exhibits dispersion due to the fact that light does not interact simply at the surface, but rather penetrates below the surface while being reflected or absorbed. (Actually, what we are interested in is the dielectric constant of the material, which is dispersive. The complex refractive index (bending power + absorption) is proportional to the square root of the dielectric constant). The second property that we can consider is the scatter of light within a material. The scatter of light within a material can be described in several different ways, but in all cases, the nature of scatter is also wavelength dependent. Blue light scatters differently than red light. All materials will scatter light to some degree, even apparently clear glass. By performing sensitive spectrophotometric measurements of the light scattered by a material (or coating) and comparing the minute biases in where the blue light is scattered relative to the red light it is possible to



determine the physical makeup and structure of the material. Energy must be conserved. So, by understanding the characteristics of the illumination energy and measuring the characteristics of the light returning from a material, we can solve increasingly complex models for determining the makeup and structure of materials. Light can only be reflected, refracted, scattered, or absorbed, and energy must be conserved. (There are many other ways in which light can interact with material and other issues such as polarization which could be considered and discussed, but for simplicity sake we will forego those for this discussion. The special case of interference does arise and is considered later when addressing some special effects pigments).

Perhaps the simplest model we can employ is derived from electromagnetic theory and is called Effective Medium Theory. Effective Medium Theory simply states that no matter how complex the coating or material, we will treat it as a single homogeneous material. A material described with 3 layers and 9 ingredients is treated as if it is a single material that is a weighted average of the ingredients, weighted by their distribution through the layers, the thickness of the layers, and the structure of the boundary between two adjacent layers. A processed material of a given formulation (recipe of ingredients and defined layer structure) will be characterized by its unique dispersive scattering properties. If anything changes in the formulation, those unique properties will change. Even if the distribution of mean particle size changes, the unique scatter properties will change.

Along with Effective Medium Theory, one of the simplest methods for characterizing the scattering behavior of the light is to consider where the light is being scattered relative to reflecting / emerging from the sample in some coordinate system. We can represent this as a bias, forward/backward and side to side with the magnitude corresponding to the light energy that is not absorbed. The more light that is scattered / reflected into a given direction, the greater the magnitude. If we then do this for each wavelength, we can then analyze the dispersive nature of the material / coating. Using this analogy, a material that is uniformly reflective at all wavelengths and uniformly scatters into all directions will exhibit no bias in any direction. A material which closely approximates this behavior is Spectralon™ (also known as Fluorolon™). Spectralon appears uniformly diffuse white under all illumination geometries and from all observation angles. There is no shine or gloss to well prepared Spectralon, even at very high grazing incidence angles. The easiest way to compute the bias of the energy is to represent each observation angle as a fixed vector, drawn from the center of the sample to

the center of the spectrometer entrance pupil. One vector is created for each wavelength and each observation angle, with magnitude the amount of energy measured. The bias is then simply derived by a vector summation of all observation angles, wavelength by wavelength, resulting in a single bias vector for each wavelength. This process of applying an Effective Medium Theory assumption together with a vector summation computation provides the necessary characteristic discrimination.

Existing industry standards for measuring plastics consist of spherical or in-plane goniometric spectrophotometer measurements. The problem with this approach is that today's complex plastics are 3 dimensional in nature. The contribution of the material structure to perception changes in the out of plane direction. Traditional in plane geometries and single camera systems do not account for the fact that perceptual effects such are goniometric in nature. They change with varying illumination and observation conditions. We do not measure gloss and haze. These are perceptual effects. We can only measure the scatter and reflection of the light with the material. Because the resulting BRDF (BSSRDF) varies multidimensionally, so will the perceptual effects such as gloss and haze.

Because in plane only geometries and single camera systems fail, it was necessary for us to develop a platform that included out of plane geometries. Industry needs for correlation to these legacy in-plane systems however, necessitated the need for incremental improvements to the existing architecture, rather than more radical approaches. Furthermore, the realities of handheld measurement devices such as the time for measurement, platform stability, etc., ruled out more robust solutions such scanning goni spectrophotometers. Cost and measurement time/stability considerations drove us to perform experiments to determine the minimum number of out of plane sample angles necessary to achieve our goals of providing direct process and formulation related information. Designs of Experiments were set up involving variations on thermoplastic injection molded panels with difference formulations and processes. Panels were created and measured using a scanning goniometric spectrophotometer. The results were analyzed and mathematical lobes fit to the results. From this we determined the sampling geometry for our hardware platform. In addition to the traditional 5 angle in plane geometry we added two additional in plane sampling angles and four out of plane angles. To further increase data density and robustness, we also added a second illuminator, thus effectively doubling the measurement results without doubling cost or complexity. See Figure 3.

Based on the descriptions given above, we fabricated several systems and repeated our Designs of Experiment on a larger basis using more formulation and process variations with finer increments.



The raw data was processed using our spectral vector summation methodology. This method is consistent with effective medium theory principals for summarizing multiangle spectral data into a two or three dimensional spectral representation. The method is a weighted vector sum of the measurement directions, with the weights being the reflectance factors for each direction. The result of this sum is a spectrum of points in 3D space, one point for each measured wavelength.

The weighted vector sum is also scaled by the length of the vector sum of an ideal white Lambertian reflector, in order to make the values reasonably comparable to typical reflectance values. The coordinate system for the results consists of the specular direction (z axis), the projection of the illumination direction orthogonal to specular (y axis), and the cross product of these two directions (x axis). We will call this result the xDNA spectra.

The xDNA vector sum is a sum of the detector direction vectors, scaled by the reflectance in each direction, as well as an additional weight factor in each direction. The optional weight can be used to restrict the vector sum to certain directions, to emphasize particular directions, or to correspond to the energy present in each direction. All data presented in this paper will only use a single illuminator (the traditional 45 degree) and the 10 diffuse (non specular) channels.

The effect of equipment settings is, of course, specific to the particular application equipment. Thus, while two samples may have xDNA spectra with the same shape, and therefore be classified as process differences, there is no purely optical criterion that can classify whether the difference is due to different settings on the same equipment, different application equipment, control additives, humidity differences, or other conditions that affect the application process. To determine the equivalence of shapes of xDNA spectra, we use the linear operations of translation, rotation, and scaling. All transformation operations are performed relative to a standard. The translation vector, rotation matrix, and scale factor are computed together, using a Procrustes algorithm to compute a least squares fit of the transformed sample xDNA spectrum to the standard xDNA spectrum. For purposes of comparison to the standard, the intermediate results of the translation and rotation operations are additionally translated to be centered at the standard's center.

Rotation

The rotation of the translated spectrum xDNA_t is denoted xDNA_a. Rotation is typically a characteristic that is coupled both to changes in process and recipe distribution. For example in a molding process rotation is a result from a change in process that results either in

a molecular weight distribution change in the size of particles in a recipe, or a change in orientation of particles due to these changes.

It is not always obvious which of the aligned spectrum xDNA_a or the scaled spectrum xDNA_s values better detects formulation differences. In some situations, two samples that differ only in process conditions have significant differences in their aligned spectra xDNA_a, so examining the scaled spectra xDNA_s is needed to determine that the difference between samples is in fact a process difference, not a formulation difference. On the other hand, it is not too hard to come up with cases in which xDNA_s could be very small for samples with noticeable formulation differences, such as different diffuse grays.

Continuing along the biological analogy, we can consider the relationship between the untransformed xDNA spectrum and the scaled xDNA_s spectrum to be somewhat like the relationship between the phenotype and genotype of a living being. Just as the phenotype of a living results not just from its genetic makeup, but also from its interaction with its environment, the xDNA of a surface results from both the underlying material, characterized by xDNA_a, and its interaction with its environment, represented by application process conditions. In considering xDNA transformations, we want to keep in mind both the transformed spectra, as well as the transformation parameters. No single number can capture all of the information of interest in these situations. Keep in mind that the reason to use indices or other single values such as color difference formula is that their simplicity and the amount of information they do provide makes up for the information that is lost when going to a single value.

We describe difference Formulas that generalize colorimetric functions and difference Formulas to xDNA coordinate data. Also considered are Formulas that use reflectance data directly, and applications of all these formula to spatially transformed xDNA data.

The DF Formula

Just as one derives colorimetric data from spectral data using illuminant and observer weighting functions, CIELAB functions, and DE*, DE₉₄, DE₂₀₀₀, and other weighting functions, one can derive colorimetric data from 3D xDNA spectra. Among the possible approaches to generalizing color difference Formulas to higher dimensional spectra are these:

1. Compute colorimetric data such as XYZ, LAB, and difference Formulas on each of x, y, and z planes. Combine difference Formulas computed on the different planes as the square root of the sum of the squares of the single plane difference Formulas.
2. Compute XYZ data on each of x, y, and z planes. Use these values as the x,y,z components of vector valued X, Y, and Z data, then compute the magnitude of the three dimensional X, Y, and Z vectors. Now compute L, a, b and color difference data using the one dimensional X, Y, and Z magnitudes.



We use the notation DF for the color difference formula computed by generalizing ordinary Delta E with approach 1. The xDNA curve may be the raw xDNA curve, or one of the transformed curves xDNA_t, xDNA_a, or xDNA_s. We use DF_t, DF_a, and DF_s for the results of computing DF on transformed curves.

As colorimetric functions were constructed to approximate human perceptual differences, DF is not necessarily the optimal difference formula to apply to transformed xDNA spectra such as xDNA_t, xDNA_a, and xDNA_s. Still, the above approaches to generalizing difference formula work just as well on transformed spectra as on untransformed xDNA.

Discussion of data and results

Below, we present a series of examples of increasing complexity. The results shown below utilize a single illuminator (45 degree incidence angle) and the 10 non specular angles as shown in figure 3. Because xDNA essentially represents the bias of the energy, we start by presenting a sample with essentially no bias.

Spectralon™

Spectralon is a diffuse white material with essentially a hemispherical BRDF. Its reflectance is 99.1% across the visible spectrum and diffuse for all angles. Because the BRDF is uniform in all directions and for all wavelengths, the vectors will all be equal. In this case, all 31 wavelength results will lie on top of each other. Figure 4a and 4b show the results. In these plots (and later) the z axis is shown vertical, y is horizontal, and x is into the paper. Recall that the z axis corresponds to the specular direction, y to the illumination direction, and x is out the side of the instrument. Note that Figure 4b is the same result as 4a but with the axis plotted on a different scale. The minute differences shown in figure 4b are a result of the wet sanding process of the Spectralon. Figure 4c shows the result of adding Black pigment to Spectralon with resultant sample reflectances of 99.1, 80, 60, 40, 20, 10, 5 and 2% shown.

Ceramic Tile

Figures 5a and 5b show the results of a series of measurements performed on a series of gray scale ceramic tiles. Reflectance values include 1%, 3.5, 15, 32, 50, and 88% respectively. Note in plot b the wavelength by wavelength out of plane bias due to the thin fired glaze layer on the tile. This is absent from the spectralon samples.

Red and Green BCRA Tiles

Figure 6. shows Red and Green BCRA Tiles. Figure 6a shows the Red xDNA. Figure 6b shows the Red raw spectral reflectances. Note again the left to right out of plane bias. However, as opposed to the white tiles, this one does not oscillate wavelength by wavelength. Figures 6c and d are for the green tile respectively. In this case, the out of plane bias forms a loop, albeit on a small x scale.

BASF Organic Dyes in Polypropylene Samples

Figure 7 shows a series of different Polypropylene formulations with 100% organic pigment, 99.5% organic pigment 0.5% black pigment, 30% organic pigment with 70% White, 15% Organic 85% White, 8% Organic Pigment with 92% White, and 2% Organic Pigment and 98% white. The organic dyes include Violet K5011, Blue K6330, Green K9360, Yellow K0961 HD, and Red K3911 HD

Samples

Figure 8 shows the BASF organic dyes in full concentration cross spectrum in xDNA space.

Samples

Figure 9 shows views in xDNA space plotted across surface texture

Samples

Figure 10 shows Gray Scale formulations in same concentrations but using Black and White pigments

Conclusion

We have presented a novel combination of spatial under sampled BRDF (including out of plane geometry) and a simplistic phenomenological model that captures both nanoscale and micro scale formulation contributions as well as process related contributions to overall appearance. We presented a preferable spectrophotometric sampling geometry as well as examples of formulation, lot to lot distribution variations, process variations, and separability of contributors. We presented a method we call xDNA and metrics derived from it for reducing the dimensionality of the data while preserving critical goniometric relationships between perceptual effects such as coarseness and sparkle and process and formulation differences.

Future work and actions

We continue to extend our research and development efforts into more robust handheld appearance measurement and communication. Logically our next steps will extend towards spatially distributed measurements, computation, model representations, and communication tools.



References

QED: The Strange Theory of Light and Matter, Richard P Feynman, Princeton Science Library, 1971

Zur Elektrodynamik Bewegter Körper, Albert Einstein, Annalen der Physik, 17, 1905

Multiple Scattering Processes, Harriet Kagiwada, Addison Wesley Publishing, 1975

Farbenphysik Fur Industrielle Anwendungen, Georg A. Klein, Springer Verlag, 2004

Light and Matter, Yehuda B. Band, Wiley, 2006

Radiative Transfer, Chandrasekhar, Oxford Univeristy Press, 1960

A novel technique for analysis of electromagnetic scattering from microstrip antennas of arbitrary shape, Uckun, S.; Sarkar, T.K.; Rao, S.M.; Salazar-Palma, M., Microwave Theory and Techniques, IEEE Transactions on, Volume 45, Issue 4, Apr 1997 Page(s):485 – 491

A vector inverse algorithm for electromagnetic scattering, Borden, B. U.S. Naval Weapons Center, China Lake, CA) SIAM Journal on Applied Mathematics (ISSN 0036-1399), vol. 44, June 1984, p. 618-626. 1984

Electromagnetic Scattering by a System of Dielectric Spheres Coated With a Dielectric Shell, Hamid, A. K. ; Hussein, Mousa I. ; Hamid, Michael, UNIVERSITY OF SOUTH ALABAMA MOBILE, NOV 2003

Fast analysis of electromagnetic scattering from finite strip gratings on a grounded dielectric slab, Valero, Alejandro; Rojas, Roberto G. , Radio Science, Volume 35, Issue 6, p. 1307-1314 (RaSc. Homepage) , 2000

A Numerical Solution for Electromagnetic Scattering from Large Faceted Conducting Bodies by Using Physical Optics-SVD Derived Bases, Gianluigi TIBERI1, Agostino MONORCHIO1, Giuliano MANARA1 and Raj MITTRA2, IEICE Transactions on Electronics, Vol E90-C, Number 2, pg 252-257, 2006

Finite Elements for Wave Electromagnetics, P.P. Silvester, G. Pelosi, IEEE Press: New York, 1994. ISBN 0-7803-1040-3. ix+534 pp.

Illustrations, tables and figures

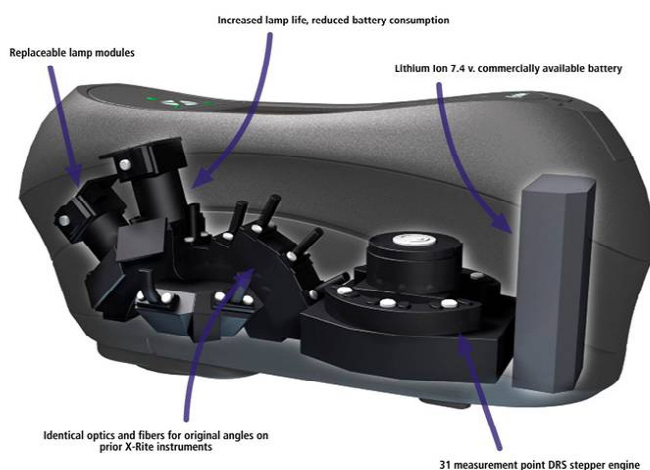


Figure 1. MA98 multi angle – out of plane gonio spectrophotometer

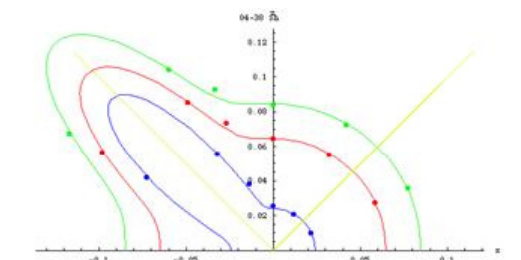
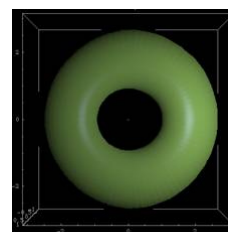
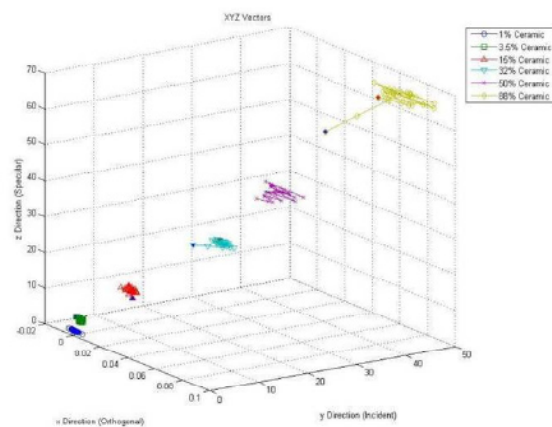
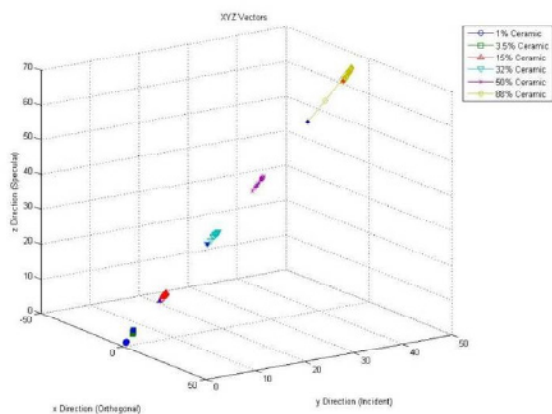


Figure 2. Figure of BRDF model fit to multi-angle measurement and the corresponding surface rendering



Figures 5a. and 5b. show the results of a series of measurements performed on a series of gray scale ceramic tiles Reflectance values include 1%, 3.5, 15, 32, 50, and 88% respectively

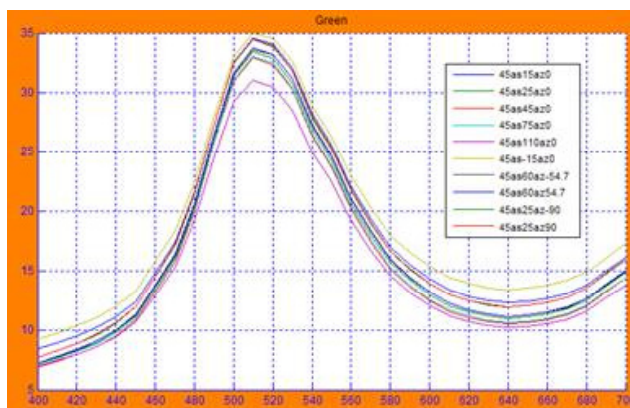
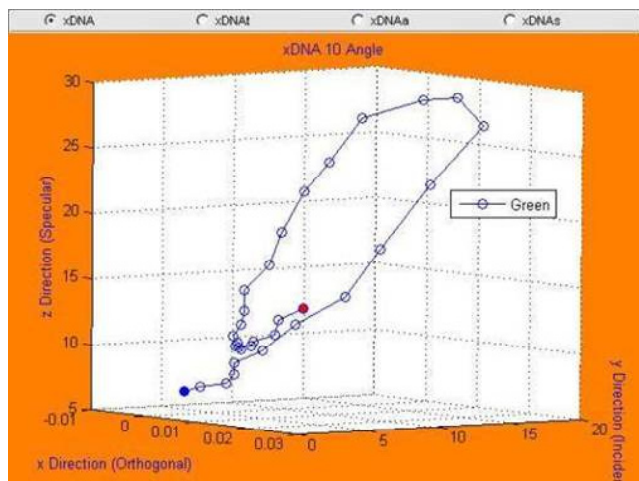
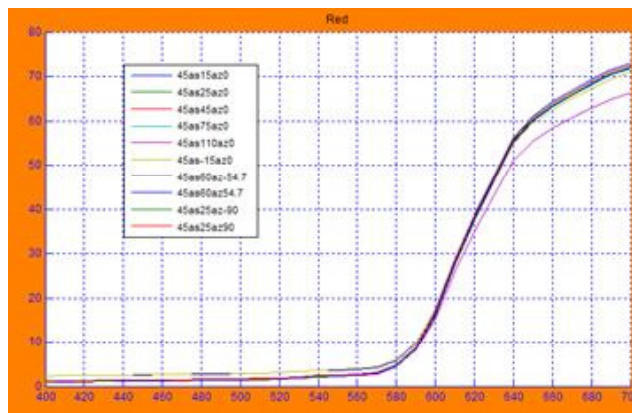
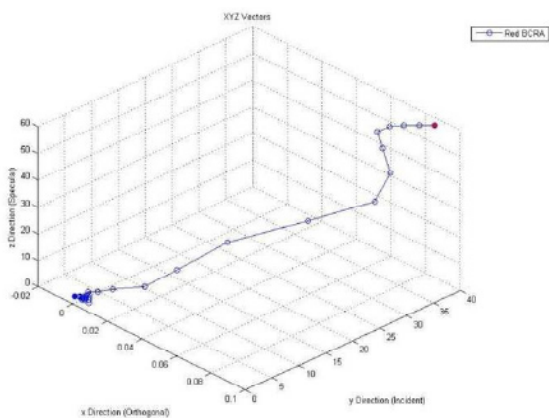


Figure 6. shows Red and Green BCRA Tiles. Figure 6a show the Red xDNA. Figure 6b shows the Red raw spectral reflectances. Figures 9c and d are for the green tile respectively.

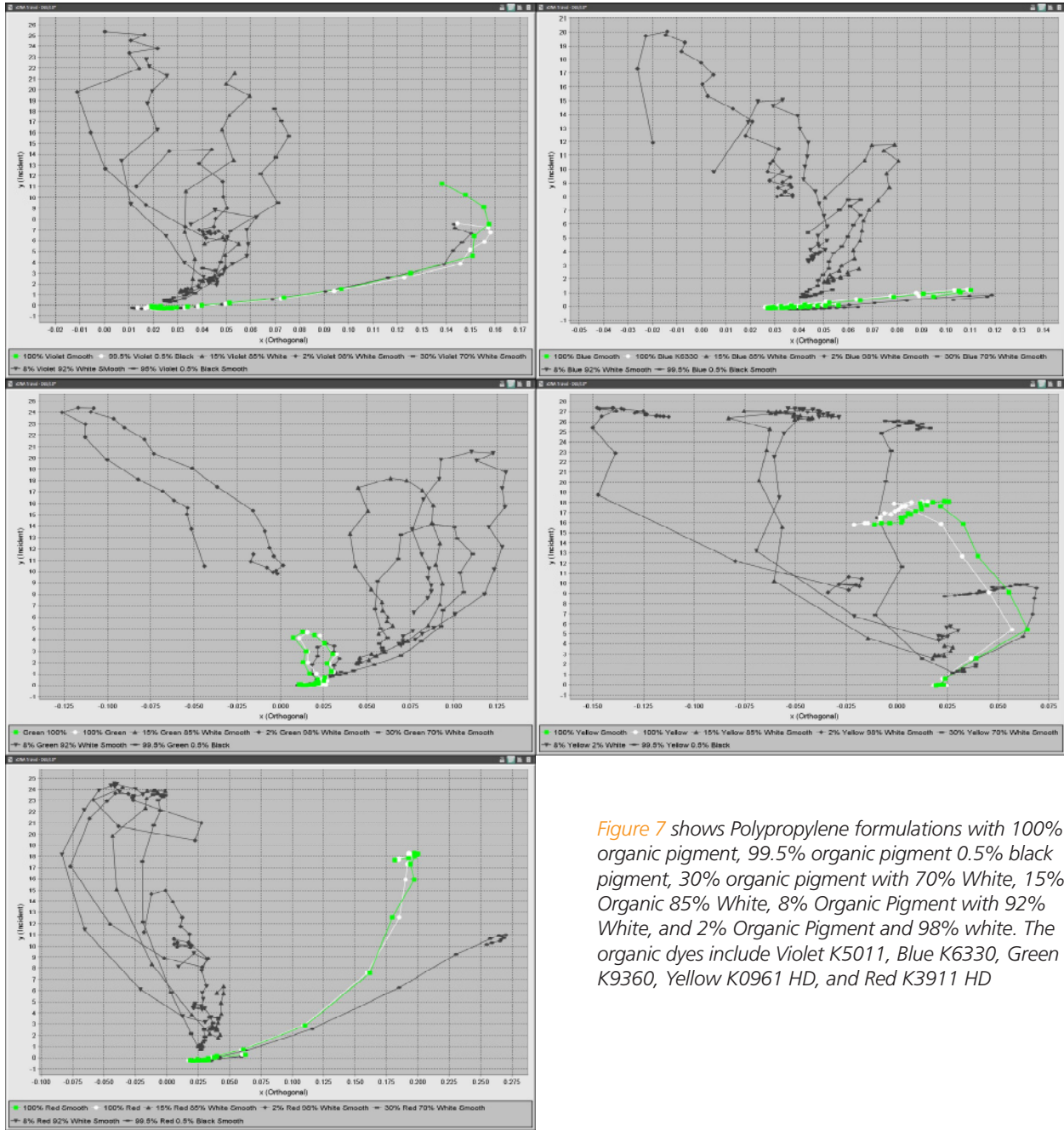


Figure 7 shows Polypropylene formulations with 100% organic pigment, 99.5% organic pigment 0.5% black pigment, 30% organic pigment with 70% White, 15% Organic 85% White, 8% Organic Pigment with 92% White, and 2% Organic Pigment and 98% white. The organic dyes include Violet K5011, Blue K6330, Green K9360, Yellow K0961 HD, and Red K3911 HD

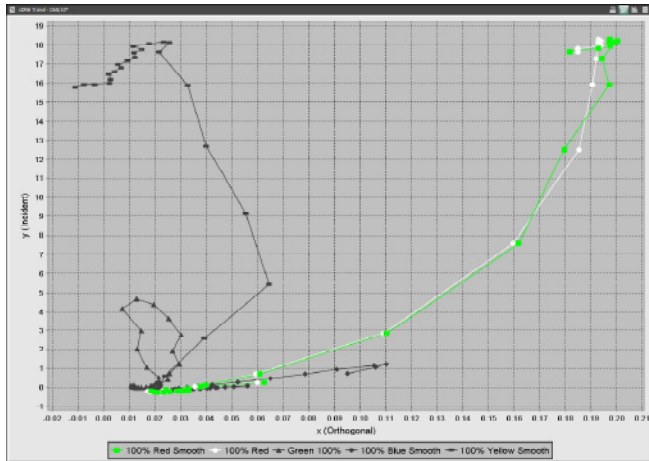


Figure 8 shows the BASF organic dyes in full concentration cross spectrum in xDNA space.

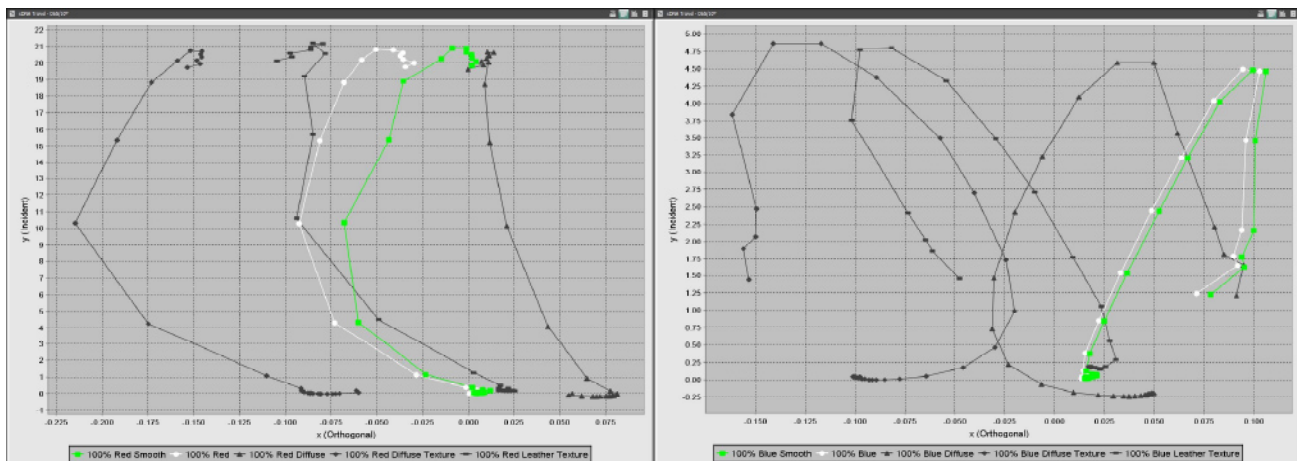


Figure 9. shows views in xDNA space plotted across surface texture

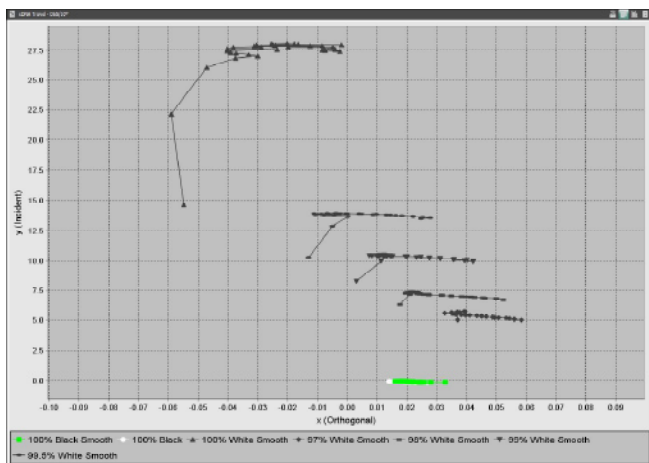


Figure 10 shows Gray Scale formulation in same concentrations but using Black and White pigments

